

A Novel UWB Flexible Antenna with Dual Notch Bands for Wearable Biomedical Devices

M. Dilruba Geyikoglu (✉ dilruba.mdk@gmail.com)

Atatürk University

Research Article

Keywords: airbrush printing, dual notch, flexible antenna, UWB, wearable biomedical devices

Posted Date: June 14th, 2022

DOI: <https://doi.org/10.21203/rs.3.rs-1718816/v1>

License:  This work is licensed under a Creative Commons Attribution 4.0 International License.

[Read Full License](#)

Abstract

This study presents a novel UWB flexible antenna with dual band-notched design for wearable biomedical devices. The proposed antenna is designed on Kapton Polyimide-based flexible substrate. This includes a CPW fed circular and triangle structure. The dual notched bands are realized by using two triangular-shaped defected ground structures. The first notched band (2.4–3.7 GHz) is generated for rejecting WLAN and WiMAX, the second notch (5.15-5.725 GHz) is generated for rejecting HyperLAN /2. The designed UWB antenna has approximately a bandwidth of 150% (2.05-14 GHz) in simulation. Thus, the designed UWB antenna meets FCC standards. The antenna has an omnidirectional radiation pattern with a maximum gain of 12.7 dB in 8.4 GHz. The proposed antenna is fabricated with the low-cost airbrush printed technique. In this technique, a higher gain value is obtained by controlling the thickness of the conductive layer. Effect of flexibility on the antenna performance is tested for different configurations in the simulation and anechoic chamber environments. According to the results obtained, the overall performance is not affected except for the shift in frequency. Since the antenna has a UWB structure, the frequency shift that occurs in bending is at a tolerable level. The proposed UWB antenna is suitable for wearable biomedical devices, with a high UWB performance.

1) Introduction

Nowadays, the health sector is based on "the right treatment for the right person at the right time." It is expressed as a personalized service according to the biological, social, and cultural characteristics of the individual. However, the Covid 19 pandemic has shown that facilitating access to treatment in the health sector and increasing the quality of treatment with the introduction of remote patient follow-up systems are the basic needs that are expected to be met. These needs will increase both the demand for wireless devices with the developing technology and the demand for wearable biomedical devices for health monitoring systems in the health sector.

Wearable biomedical devices are popularly used, especially in body-centered systems. For this purpose, the need for flexible antennas that can be applied in biomedical applications, wearable applications [1, 2] and body-mounted applications has increased. [3–5]. Various antennas are used for wireless communication in clinical treatment and remote monitoring devices. Antennas typically need to be flexible, highly efficient to facilitate all on-body wireless systems. It is also highly desirable to maintain a reliable connection, as deformation and body movement is likely to occur in a real-time operation, which will degrade antenna performance. Much attention has been directed to wearable systems, wearable antennas and antenna miniaturization techniques in the literature [6–9].

The need for wide bandwidth, high data rates, low cost of implementation, miniature dimensions offer the opportunity for UWB (the range from 3.1 GHz to 10.6 GHz [10]) to be widely used for future wireless technology. But, UWB communication systems have serious electromagnetic interference problems due to the fact that there are many narrowband wireless communication systems operating in the same frequency spectrum such as WLAN, Wi-MAX, HyperLAN /2 bands etc. These interferences can be

overcome by adding bandstop filters to the UWB antennas. However, its increases both the complexity of the UWB system and the cost. Therefore, these interference effects can be reduced with an antenna band-notch characteristic. Many trends in the design of UWB antennas have been reported in recent years [11–13]. However, designing flexible antennas for wearable applications requires constant innovation [14]. Different planar monopole antenna structures are widely used in the design of UWB antennas because they show fixed omnidirectional patterns on the UWB frequency band. Designing a flexible antenna will require thin substrates; as a result, the antenna will tend to degrade in the radiation pattern. It is an element to be considered in the design. The comparison of current studies in the literature is given in Table 1.

Table.1 The flexible UWB antenna literature comparison.

Ref.	Operating range (GHz)	Bandwidth (%)	Efficiency (%)	Number of Notch band	Peak Gain (dBi)	Bending test
[15]	2.7–12	126	55–86	Dual	8.2	No
[16]	1.2–13	166	70–82	Triple	6	Yes
[17]	2.7–12	126	-	Dual	5.2	No
[18]	3.1–11	112	-	Dual	5	No
[19]	3.1–10.6	109	-	Single	3	Yes
[20]	2–6	100	-	Triple	3.75	Yes
[21]	2.76–10.6	117	-	Dual	-	No
[22]	3.6-19.08	136	-	Single	3	No
[23]	3–12	120	-	Triple	5.2	No
This work	2.05-14	150	73–94	Dual	12.7	Yes

This article has presented the design and realisation of a flexible UWB antenna with dual-band rejection capabilities for wearable biomedical devices. The dual notched bands are realized by using two triangular-shaped defected ground structures (DGS). The designed antenna has a simple structure with few geometric parameters. The antenna is tested for different bending scenarios. According to the results, the overall performance has not been affected except for the drift in frequency. Due to its excellent features such as high gain, bandwidth, omnidirectional radiation pattern and interference rejection ability, the proposed UWB flexible antenna is suitable for wearable biomedical devices.

2) Antenna Design

For wireless network systems to adapt to the developing technology, there has been a need to improve antenna designs. The planar monopole antenna structure is widely used in UWB systems because it shows advantageous antenna performance characteristics such as easy configuration, wide bandwidth, high efficiency. It is the antenna structure that is frequently preferred in wearable applications. The monopole antenna was designed using a circular patch and DGS triangular form fed by CPW. The proposed antenna uses a flexible Kapton ($\epsilon_r = 3.5, h = 0.125 \text{ mm}, \tan \delta = 0.002$) substrate with mm^3 dimensions as shown in Fig. 1. The proposed architecture has been successfully tested and developed with a wide bandwidth of 150 % of the UWB frequency. To achieve better impedance matching in the design, triangular ground structures are designed. The detailed dimensions of the proposed antenna are shown in Table 2. The radius of the initial circular structure is estimated using Eqs. 1 and 2[24].

$$f_r = \frac{1.8412 \times c}{4\pi R \sqrt{\epsilon_r}} \text{ Eq. (1)}$$

$$R = R_b \left(1 + \frac{2h}{\pi \epsilon_r R_b} \left[\ln \left(\frac{\pi R_b}{2h} \right) + 1.7726 \right] \right)^{1/2} \text{ Eq. (2)}$$

where f_r is the center frequency, ϵ_r is substrate permeability, h is substrate thickness, b is variable index and R is average effective radius.

A square-shaped DGS resonator slot is added to the ground plane of the CPW antenna for the notch band-reject (Fig. 1-b/1-c). The operation resonance frequencies of the DGS resonators depend on their physical dimensions [25]. A decrease in the total length of the DGS resonator will decrease the inductance while an increase in the width of the DGS resonator decreases its capacitance. According to this operating logic, the DGS resonator acts like the parallel capacitance inductance circuit. The dimensions of the DGS slot are calculated through both the notched band (f_{notch}) frequency equation Eq. (3) and LC equivalent circuit equation Eq. (4,5)[25].

$$f_{notch} = \frac{c}{4 \left(L_t \sqrt{\epsilon_e} \right)} \text{ Eq. (3)}$$

where, L_t is slot length in DGS, ϵ_e is effective dielectric constant and c is velocity of light.

$$C = \frac{\omega_c}{2Z_0(\omega_0^2 - \omega_c^2)} \text{ Eq. (4)}$$

$$L = \frac{1}{4\pi^2 f_0^2 C} \text{ Eq. (5)}$$

where C is the capacitance, ω_0 is the angular resonance frequency, ω_c is the cutoff angular frequency, Z_0 is the characteristic impedance, L is the inductance. The DGS length obtained for WLAN and WiMAX notch is 78.9mm, and the DGS length obtained for hyperlan/2 notch is 52.9 mm.

Table 2
The geometric parameters.

Parameters	L	L ₁	L ₂	L _g	L _f	W	W _g	W _f	C _f	R/2
Dimensions (mm)	62	9.25	18.5	3.5	7.2	60	28.9	0.8	0.7	23.8
Parameters	S ₁	S ₂	S ₃	S ₄	S ₅	S ₆	S ₇	S ₈	S ₉	S ₁₀
Dimensions (mm)	0.3	8	8.1	7.5	7.5	6.9	6.9	6.3	6.3	5.7

The reflection coefficient of the simulated results of the design steps is shown in Fig. 2. According to the results, impedance matching and operating bandwidth are effectively improved with the DGS resonator. The effect of slots on the notch band is better expressed by the surface current distribution. Figure 3 shows the surface current distribution in both without notch bands and with dual notch bands. In the left triangular ground structure, the square slot has a rather dense surface current, indicating the contribution of the larger square to reject the WLAN-WiMAX notch band. Similarly, in the right triangular ground structure, the higher surface current concentration on the smaller square indicates the contribution of the smaller square to reject the HyperLAN/2 notch band.

3) Simulation And Measured Results

Air-brush (spray printing) printing technique is used to randomly place inks with a wide viscosity range on the surface [10, 11]. The basic schematic of the production technique is given in Figure 4-a. The proposed antenna is fabricated using a Magic Brushmark airbrush and silver ink (Figure 4-b). The antenna prototypes fabricated on Kapton is given in Figure 4-c-d.

3.1) Radiation performance analysis

The produced antenna's performance parameters(reflection coefficient, radiation pattern, total efficiency, and gain) were measured in a chamber environment using the N9928A model network analyzer. VNA calibration was performed. The simulated and measured reflection coefficient of the proposed UWB antenna is shown in Figure 5. The comparative analysis of the simulation and measured results of the proposed flexible dual notch band UWB antenna is given in Table 3. The design results and the measurement results are in harmony and provide an ultra-wide operating frequency band with dual-band rejection characteristics. A horn antenna with high gain and efficiency value operating in a wide frequency range in the 2-18 GHz range has been used in this study. The measurement environment is shown in Figure 6. Antenna gain was calculated using the 3-point method. The efficiency and gain results of the dual notched antenna are plotted in Figure 7. There is more than 90% agreement between antenna gain measurement and simulation results. The notch band frequencies ranges have less than -3 dB gain performance, which provides it to reject the interference of other systems. The efficiency value measure and simulation results are harmonious.

Table.3 The proposed flexible UWB antenna results

	Peak Gain (dBi)	Efficiency (%)	-10 dB Bandwidth (GHz)
UWB (simulated)	12.72	73-94	2.05-14
UWB (measured)	12.57	71-85.2	2.05-14
UWB dual notched (simulated)	12.73	70.8-2.95	2.05-14
UWB dual notched (measured)	11.63	67.1-85.4	2.05-14





The E field and H field patterns of free space measurements both without notched and with dual notched are made in an anechoic environment. The simulation and measurement results of the antenna's E field and H field radiation patterns at 3-6-12 GHz are shown in Figure 8. It has been observed that the produced antenna shows a dipole-shaped radiation pattern in the E field and an omnidirectional radiation pattern in the H field for the frequencies examined in the UWB frequency range (3,6,12 GHz). According to radiation analysis is understood that the proposed antenna can be used for various wearable biomedical devices with its high-performance features, flexible and compact structure. The proposed antenna may be an excellent candidate to meet UWB requirements, and its compact configuration makes it suitable for all RF applications.

3.2 Bending Test:

The proposed UWB flexible antenna with dual notch bands needs to be evaluated in different configurations for potential use in devices. The antenna's flexibility is investigated experimentally by placing it on foam cylinders with different radii of curvature. The antenna in the bent form in different configurations is shown in Table 4 . Performance characteristics such as S_{11} , gain, and radiation pattern was measured experimentally to validate the simulation results, considering all configurations. Simulation and measurement results are presented in Table 4. According to Table 4, the effects of bending on the performance characteristics are reasonable, not affecting the overall performance. Both the double notch band and the UWB feature are preserved. The radiation pattern of the proposed UWB flexible antenna with dual notch bands is measured for bending radius $R=20$ mm in the vertical and horizontal positions, the results are shown in Figure 9. From the simulation and measurement bending results, it is seen that the proposed antenna structure is suitable for flexible applications for the bending radius of 10mm and 20 mm. In general, the vertical and horizontal bending configurations maintain wider impedance bandwidth with dual notch bands. In addition to bending, the foam cylinder material ($\epsilon_r=1.03$

[26] may have had a minimal effect on antenna performance. No significant deterioration in basic operating parameters was observed after testing the antenna under different bending conditions. The proposed design, structural strength, and continuity of performance characterize its usability in wearable biomedical devices.

Table.4 The proposed UWB flexible antenna with dual notch bands bending results

		-10 dB Bandwidth (GHz)	Peak Gain (dBi)	Efficiency (%)
Horizontal R=10 mm (simulated)		2.05- 14	12.72	73-91
Horizontal R=10 mm (measured)		2.05- 14	12.53	69-87
Vertical R=10 mm (simulated)		2.05- 14	11.87	74.6-91.2
Vertical R=10 mm (measured)		2.05- 14	11.65	73.2-90.4
Horizontal R=20 mm (simulated)		2.05- 14	12.63	73.5-91.4
Horizontal R=20 mm (measured)		2.05- 14	12.6	74-89
Vertical R=20 mm (simulated)		2.05- 14	11.97	67-84.2
Vertical R=20 mm (measured)		2.05- 14	11.6	66.8-83.8

4) Conclusion

A flexible dual notch band UWB antenna for wearable biomedical devices is proposed, analyzed, and measured in this study. The proposed antenna is printed on a 12.5 μm thick Kapton substrate. The design consists of circle-shaped radiating elements and square-shaped slits on the ground for achieving dual notched band characteristics. The proposed flexible antenna is fabricated with the technique of Air-Brush-printing after comprehensive performance analysis. According to measurement results, it has 150 % (2.05-14 GHz) of operating bandwidth with dual notch characteristics at 2.4 to 3.7 GHz, 5.15 to 5.725 GHz. Furthermore, the proposed antenna is tested under bending effects (flat, vertical, and horizontal) and exhibits a low susceptibility to performance degradation in terms of impedance matching and radiation pattern. The antenna's efficient performance, easy fabrication process, along with its flexibility and thin profile, suggests that it would be a reasonable candidate for integration within flexible and wearable devices in wearable biomedical devices.

Declarations

Ethics approval and consent to participate Not applicable.

Consent for publication The authors consent to publish the work upon acceptance.

Competing Interests The author declares no competing interests.

Author contributions The author conceived this project. Material preparation, data collection, electromagnetic simulations, and analysis were performed by M.Dilruba Geyikoglu.

Funding The author declares that no funds, grants, or other support were received during the preparation of this manuscript.

Availability of data and materials There are no supplementary materials, and the data is available upon reasonable request.

References

1. J. Shi *et al.*, "Smart textile-integrated microelectronic systems for wearable applications," *Advanced materials*, vol. 32, no. 5, p. 1901958, 2020.
2. G. Bailly, J. Müller, M. Rohs, D. Wigdor, and S. Kratz, "Shoesense: a new perspective on gestural interaction and wearable applications," in *Proceedings of the SIGCHI Conference on Human Factors in Computing Systems*, 2012, pp. 1239-1248.
3. C. Liu, Y.-X. Guo, and S. Xiao, "A review of implantable antennas for wireless biomedical devices," in *Forum for electromagnetic research methods and application technologies (FERMAT)*, 2016, vol. 14, no. 3, pp. 1-11.
4. R. Shadid and S. Noghianian, "A literature survey on wireless power transfer for biomedical devices," *International Journal of Antennas and Propagation*, vol. 2018, 2018.
5. V. Vakhter, B. Soysal, P. Schaumont, and U. Guler, "Minimum on-the-node data security for the next-generation miniaturized wireless biomedical devices," in *2020 IEEE 63rd International Midwest Symposium on Circuits and Systems (MWSCAS)*, 2020: IEEE, pp. 1068-1071.
6. M. Fallahpour and R. Zoughi, "Antenna miniaturization techniques: A review of topology-and material-based methods," *IEEE Antennas and Propagation Magazine*, vol. 60, no. 1, pp. 38-50, 2017.
7. D. Upadhyay and R. P. Dwivedi, "Antenna miniaturization techniques for wireless applications," in *2014 Eleventh International Conference on Wireless and Optical Communications Networks (WOCN)*, 2014: IEEE, pp. 1-4.
8. E. J. Rothwell and R. O. Ouedraogo, "Antenna miniaturization: definitions, concepts, and a review with emphasis on metamaterials," *Journal of Electromagnetic Waves and Applications*, vol. 28, no. 17, pp. 2089-2123, 2014.
9. S. M. Haque and K. M. Parvez, "Slot antenna miniaturization using slit, strip, and loop loading techniques," *IEEE Transactions on Antennas and Propagation*, vol. 65, no. 5, pp. 2215-2221, 2017.
10. Z.-C. Hao, J.-S. Hong, S. K. Alotaibi, J. P. Parry, and D. Hand, "Ultra-wideband bandpass filter with multiple notch-bands on multilayer liquid crystal polymer substrate," *IET microwaves, antennas & propagation*, vol. 3, no. 5, pp. 749-756, 2009.

11. Y. Soerbakti, R. F. Syahputra, M. D. H. Gamal, D. Irawan, E. H. Putra, and R. S. Darwis, "Improvement of low-profile microstrip antenna performance by hexagonal-shaped SRR structure with DNG metamaterial characteristic as UWB application," *Alexandria Engineering Journal*, vol. 61, no. 6, pp. 4241-4252, 2022.
12. S. Saleh, W. Ismail, I. S. Z. Abidin, M. H. Bataineh, and A. S. Alzoubi, "Compact UWB Vivaldi Tapered Slot Antenna," *Alexandria Engineering Journal*, vol. 61, no. 6, pp. 4977-4994, 2022.
13. J. Mol, S. E. Florence, and M. Abraham, "Twisted F-Shaped Slot Loaded UWB Printed Antenna for On-Body Application," *Wireless Personal Communications*, pp. 1-19, 2022.
14. S. R. Zahran, M. A. Abdalla, and A. Gaafar, "New thin wide-band bracelet-like antenna with low SAR for on-arm WBAN applications," *IET Microwaves, Antennas & Propagation*, vol. 13, no. 8, pp. 1219-1225, 2019.
15. S. Kannadhasan and R. Nagarajan, "Development of an H-shaped antenna with FR4 for 1–10 GHz wireless communications," *Textile Research Journal*, p. 00405175211003167, 2021.
16. S. Lakrit, S. Das, S. Ghosh, and B. T. P. Madhav, "Compact UWB flexible elliptical CPW-fed antenna with triple notch bands for wireless communications," *International Journal of RF and Microwave Computer-Aided Engineering*, vol. 30, no. 7, p. e22201, 2020.
17. Y. Li, W. Li, and Q. Ye, "A CPW-fed circular wide-slot UWB antenna with wide tunable and flexible reconfigurable dual notch bands," *The Scientific World Journal*, vol. 2013, 2013.
18. O. A. Safia, M. Nedil, L. Talbi, and K. Hettak, "Coplanar waveguide-fed rose-curve shape UWB monopole antenna with dual-notch characteristics," *IET Microwaves, Antennas & Propagation*, vol. 12, no. 7, pp. 1112-1119, 2018.
19. H. Yoon, Y. Yoon, H. Kim, and C.-H. Lee, "Flexible ultra-wideband polarisation diversity antenna with band-notch function," *IET Microwaves, Antennas & Propagation*, vol. 5, no. 12, pp. 1463-1470, 2011.
20. A. Zaidi, W. A. Awan, N. Hussain, and A. Baghdad, "A Wide and Tri-band Flexible Antennas with Independently Controllable Notch Bands for Sub-6-GHz Communication System," *Radioengineering*, vol. 29, no. 1, 2020.
21. X. Zhang and G. Wang, "A flexible monopole antenna with dual-notched band function for ultrawideband applications," *International journal of Antennas and Propagation*, vol. 2014, 2014.
22. Q. Zou and S. Jiang, "A compact flexible fractal ultra-wideband antenna with band notch characteristic," *Microwave and Optical Technology Letters*, vol. 63, no. 3, pp. 895-901, 2021.
23. V. Kollipara, S. Peddakrishna, and J. Kumar, "Planar EBG loaded UWB monopole antenna with triple notch characteristics," *International Journal of Engineering and Technology Innovation*, vol. 11, no. 4, p. 294, 2021.
24. D. D. Krishna, M. Gopikrishna, C. K. Aanandan, P. Mohanan, and K. Vasudevan, "Compact dual band slot loaded circular microstrip antenna with a superstrate," *Progress In Electromagnetics Research*, vol. 83, pp. 245-255, 2008.
25. S. Hekal, A. B. Abdel-Rahman, H. Jia, A. Allam, A. Barakat, and R. K. Pokharel, "A novel technique for compact size wireless power transfer applications using defected ground structures," *IEEE*

26. J. Bor, O. Lafond, H. Merlet, P. Le Bars, and M. Himdi, "Technological process to control the foam dielectric constant application to microwave components and antennas," *IEEE Transactions on Components, Packaging and Manufacturing Technology*, vol. 4, no. 5, pp. 938-942, 2014.

Figures

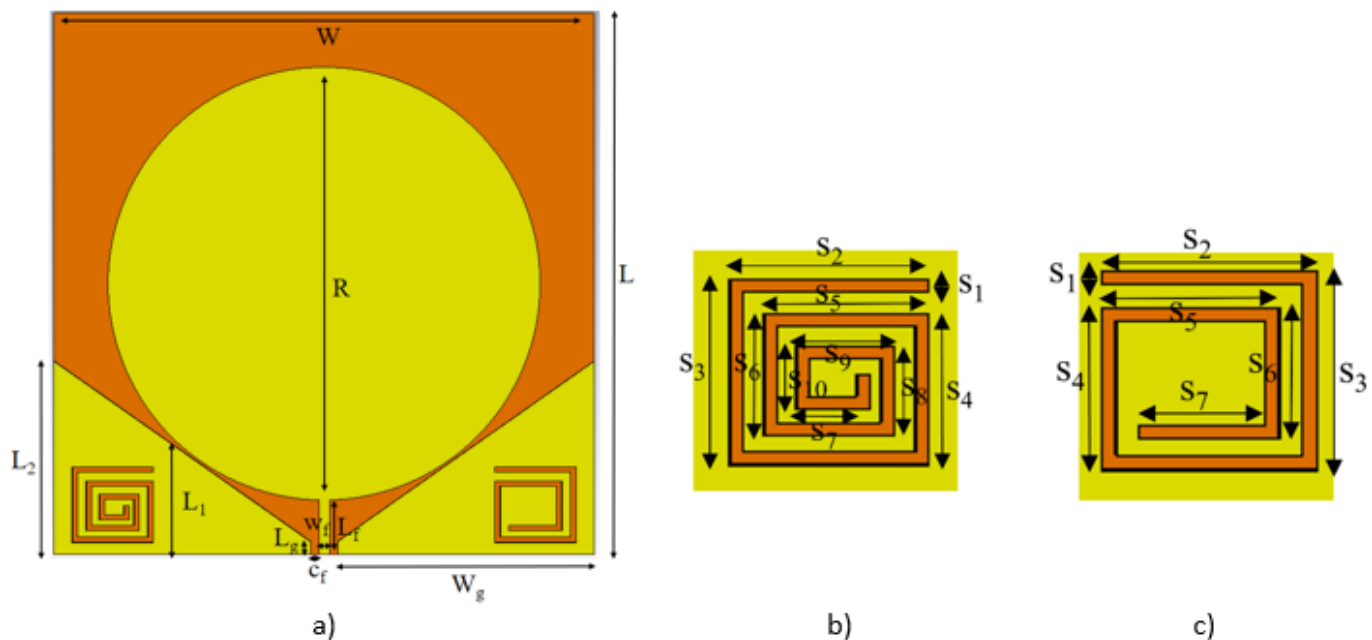


Figure 1

The antenna design schematic a) the whole antenna structure, b) the DGS resonator on the ground on the left, c) the DGS resonator on the ground on the right.

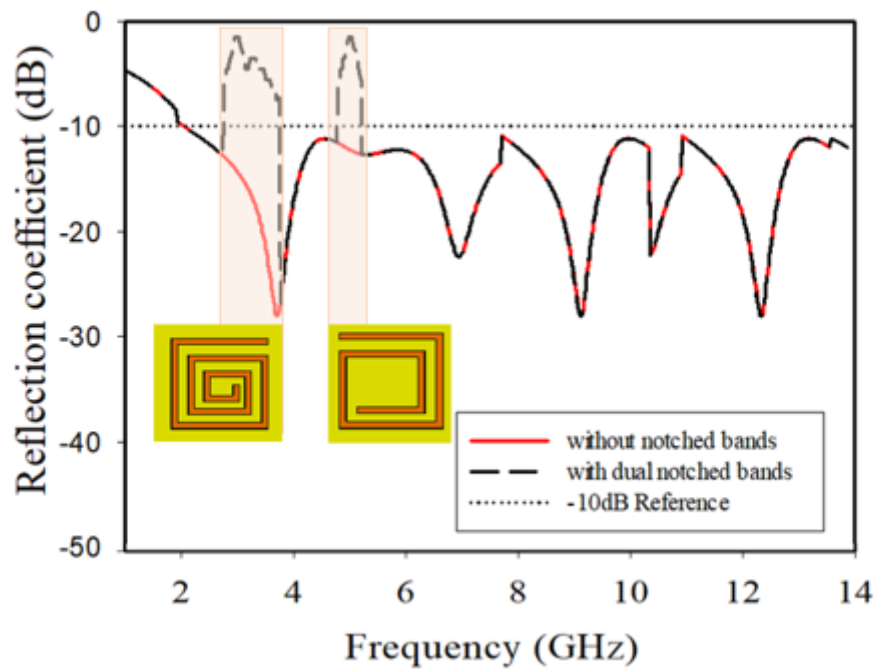


Figure 2

The simulation results of the reflection coefficient

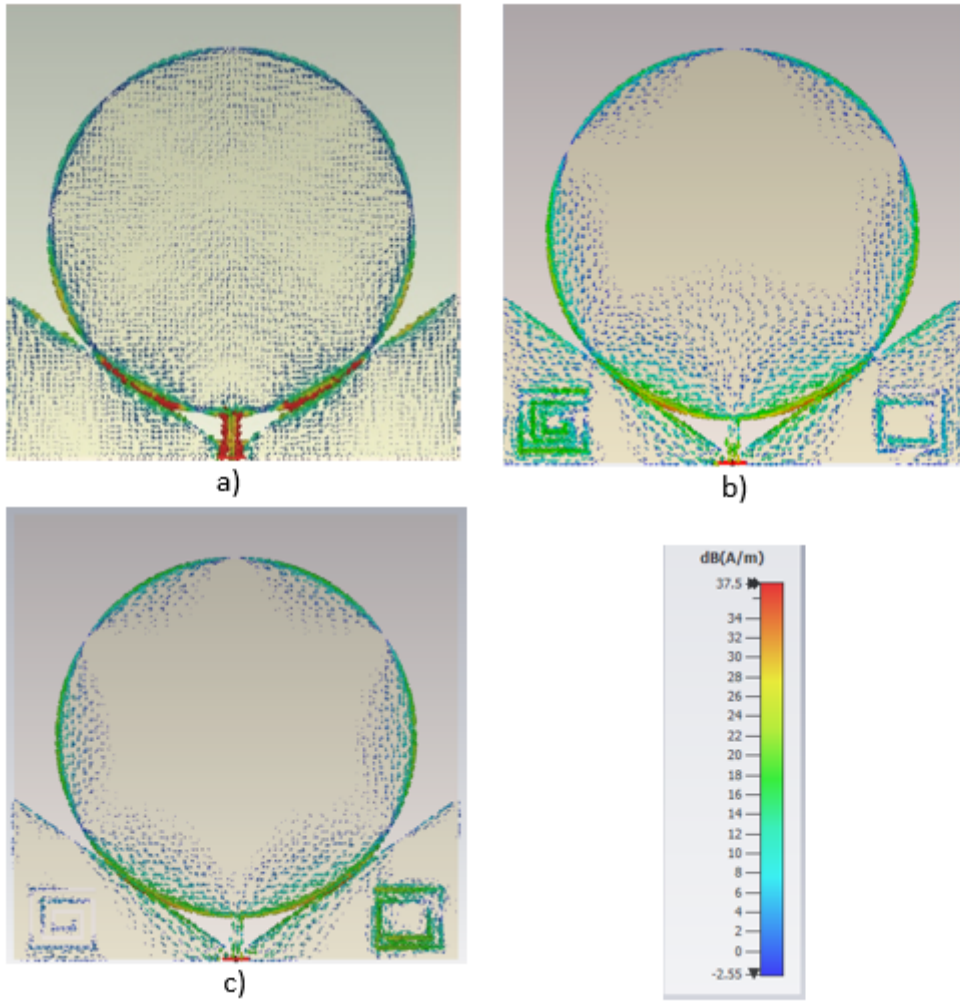


Figure 3

The surface current distributions of the proposed notched UWB antenna: a) without notch band, b) with dual notched (DGS left WLAN-WiMAX), c) with dual notched (DGS right HyperLAN /2)

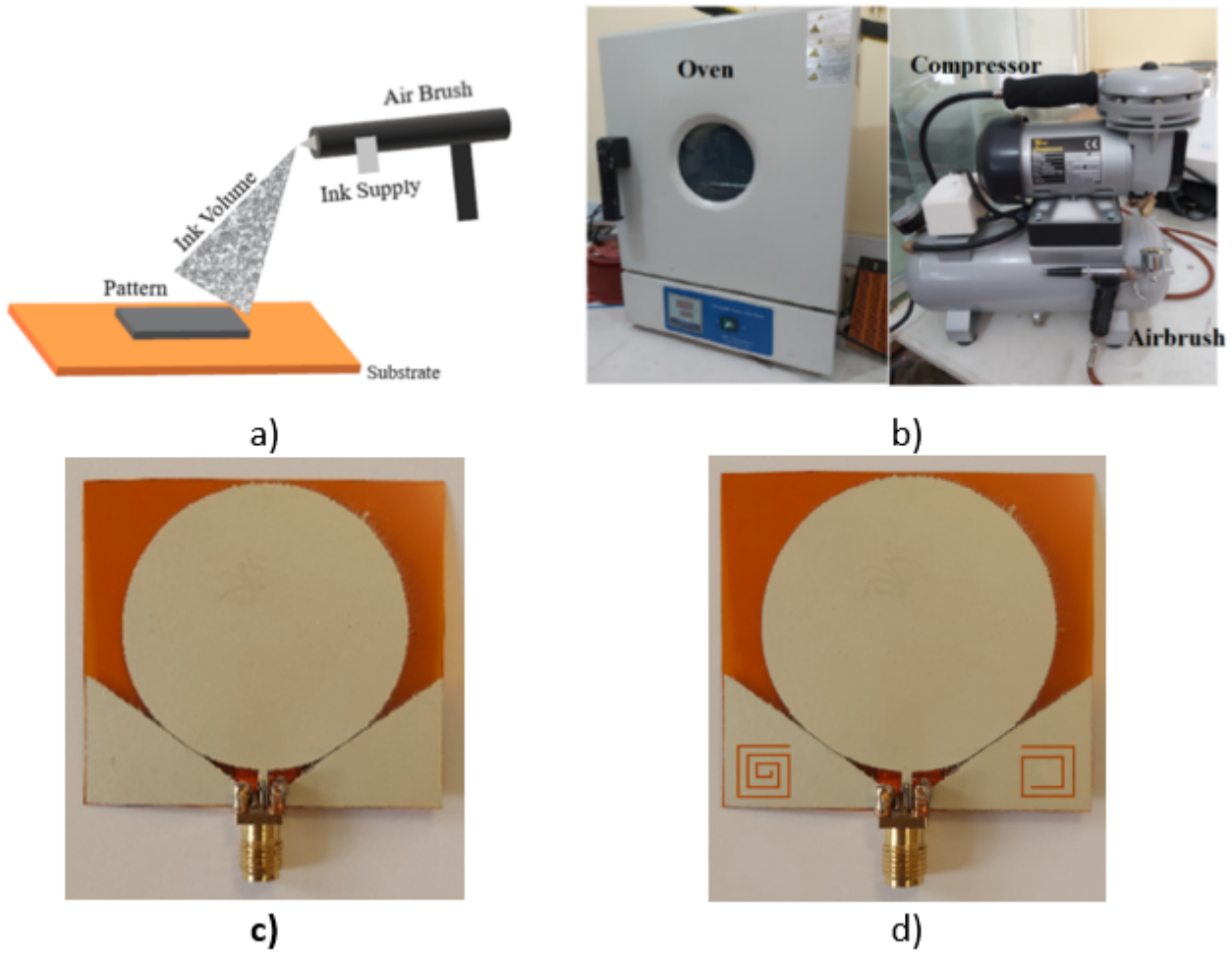


Figure 4

a) The basic schematic of the production technique b) Equipment used in production c) The conventional antenna prototype produced on Kapton d) The DGS resonators antenna prototype produced on Kapton.

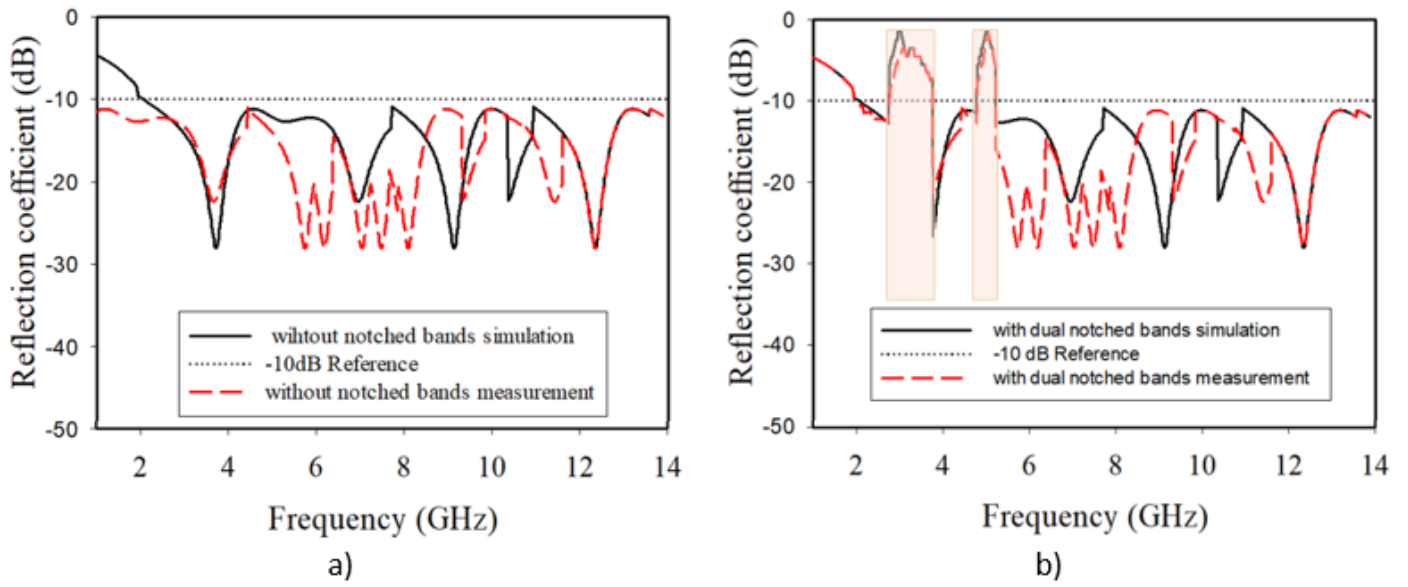


Figure 5

The results of the reflection coefficient a) without notched bands b) dual notched bands.

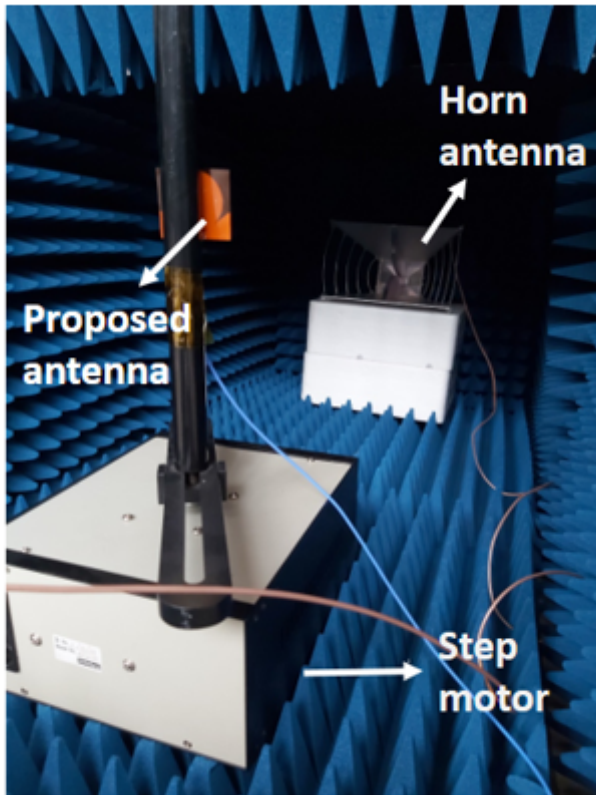
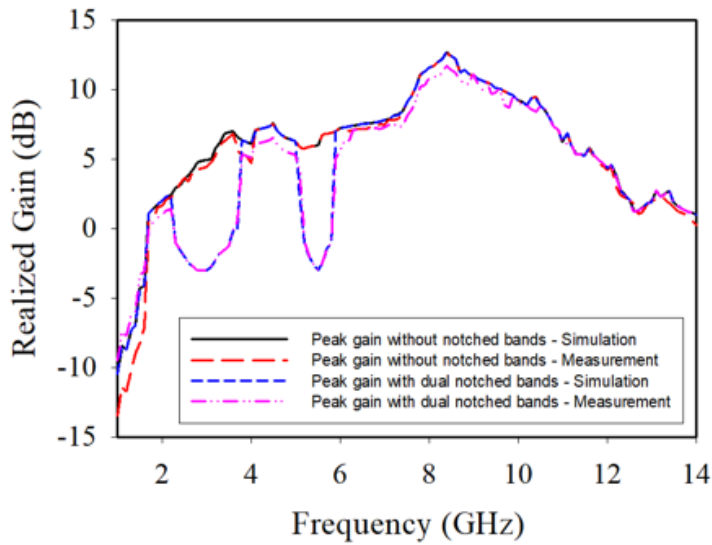
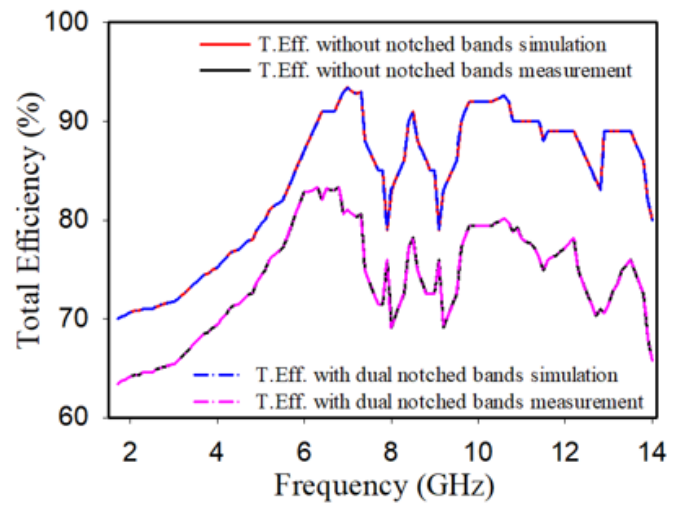


Figure 6

The measurement environment



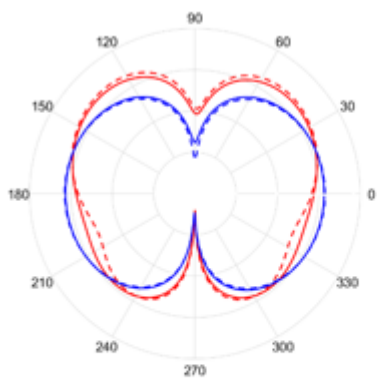
a)



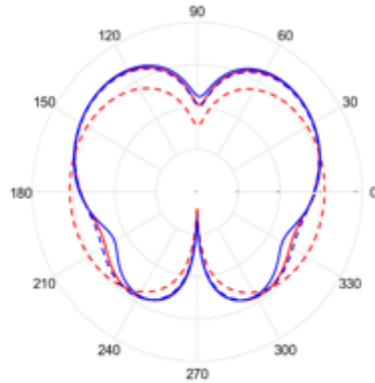
b)

Figure 7

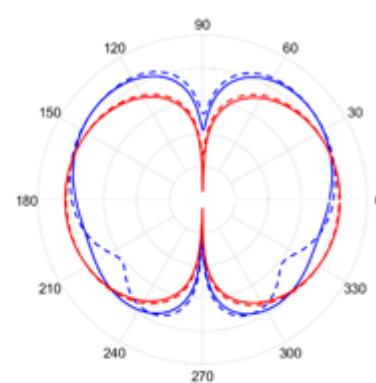
Simulation and measurement results of a) the gain b) the efficiency.



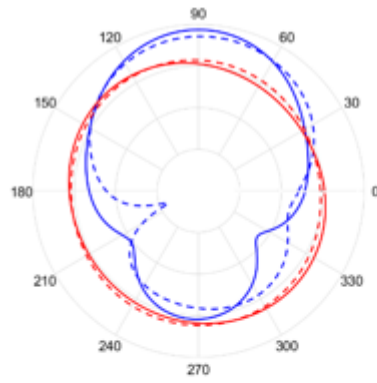
a)



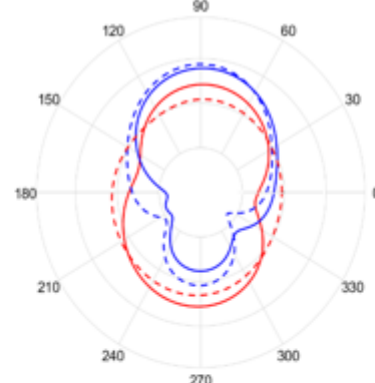
b)



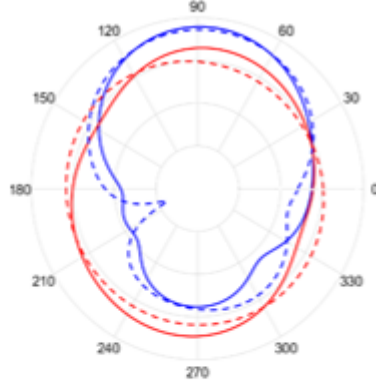
c)



d)



e)



f)

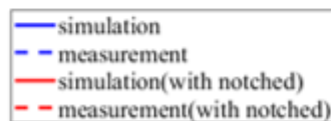


Figure 8

The simulation and measurement results of the antenna radiation pattern a) E- field 3 GHz, b) E- field 6 GHz, c) E- field 12 GHz, d) H-field 3 GHz, e) H-field 6 GHz, f) H-field 12 GHz.

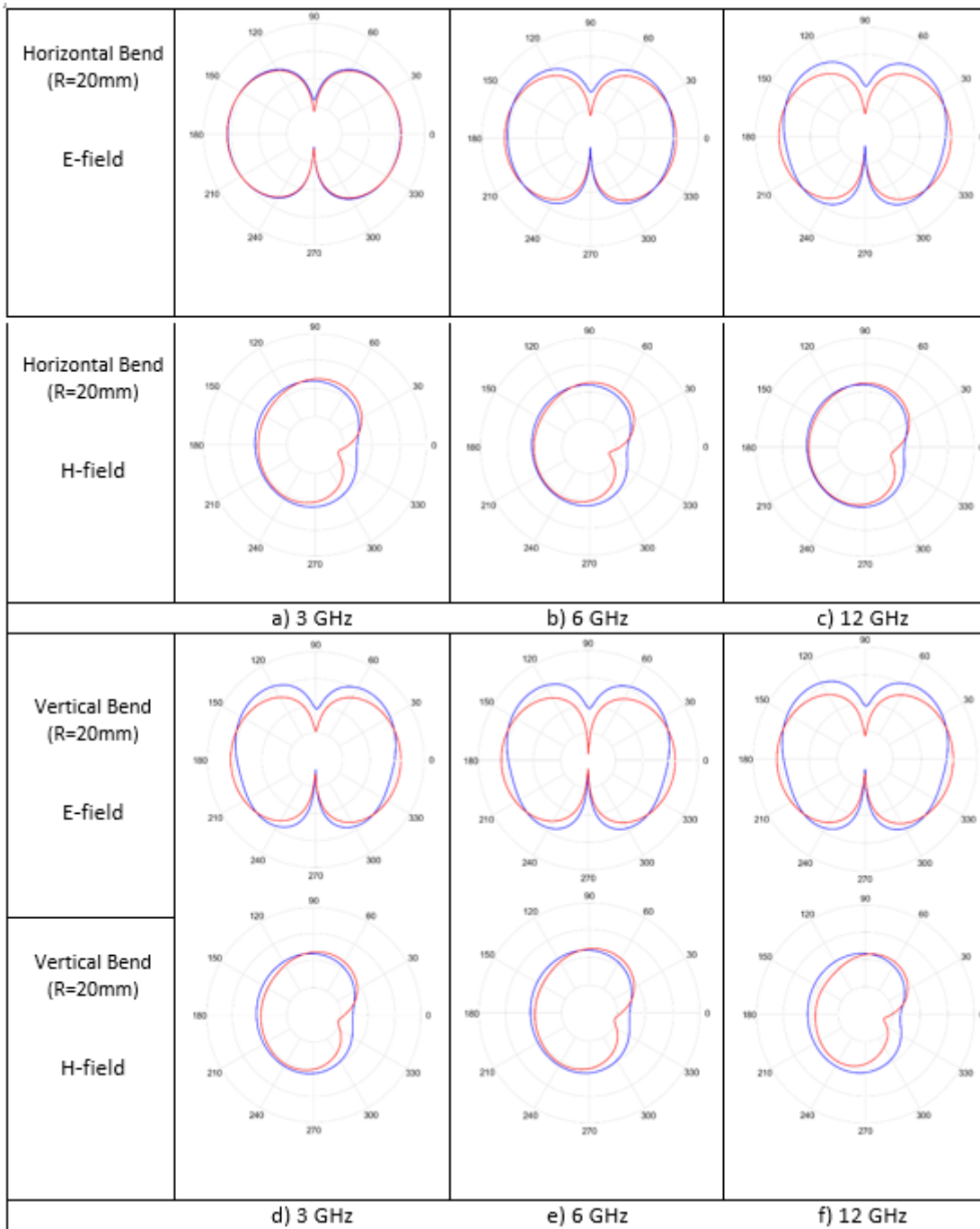


Figure 9

Measurement results of antenna radiation pattern for different bending scenarios